

Article

A Novel Computation of Delay Margin Based on Grey Wolf Optimisation for a Load Frequency Control of Two-Area-Network Power Systems

Mohammad Haziq Ibrahim ^{1,*}, Ang Swee Peng ^{1,†}, Muhammad Norfauzi Dani ¹, Ashraf Khalil ², Kah Haw Law ¹, Sharina Yunus ¹, Mohammad Ishlah Rahman ³ and Thien Wan Au ⁴

¹ Electrical & Electronic Engineering Programme Area, Universiti Teknologi Brunei, Bandar Seri Begawan BE1410, Brunei

² DTU Engineering Technology, Technical University of Denmark, 2750 Ballerup, Denmark

³ School of Science and Engineering, Politeknik Brunei, Ministry of Education, Bandar Seri Begawan BA1311, Brunei

⁴ School of Computing and Informatics, Universiti Teknologi Brunei, Bandar Seri Begawan BE1410, Brunei

* Correspondence: p20210003@student.utb.edu.bn

† These authors contributed equally to this work.

Abstract: In classical power systems, frequency measurements are transferred via a specialised communication channel, resulting in time delay. The time delay plays a major role in a power system, which can reduce the dynamic performance of the load–frequency control (LFC) system and can destabilise the system. The research to date has tended to focus on developing a new algorithm to determine the delay margin (DM) rather than looking into a hybrid algorithm which includes a nature-inspired metaheuristic optimisation technique. This paper introduces a novel method for computing the DM based on grey wolf optimisation (GWO), specifically for the constant time delay. In the proposed method, GWO is employed to optimise the minimum error of the spectral radius and to determine the best design variable of the crossing frequency. With the help of the proposed method, the sweeping range is no longer required, which improves the accuracy of the result. To evaluate the proposed method, a two-area network power system is considered as a case study. Furthermore, the effect of the PI controller gains on the DM is taken into account. The proposed method efficacy is demonstrated by comparing it with the most recently published methods. The results demonstrate that the proposed method is remarkably better than the existing methods found in the literature, where the smallest percentage inaccuracy using the simulation-based DM based on GWO is found to be 0.000%.

Keywords: communication time delay; delay margin; delay dependent stability; grey wolf optimisation; two-area load–frequency control



Citation: Ibrahim, M.H.; Peng, A.S.; Dani, M.N.; Khalil, A.; Law, K.H.; Yunus, S.; Rahman, M.I.; Au, T.W. A Novel Computation of Delay Margin Based on Grey Wolf Optimisation for a Load Frequency Control of Two Area Network Power Systems.

Energies **2023**, *16*, 2860. <https://doi.org/10.3390/en16062860>

Academic Editor: Attila Magyar

Received: 15 February 2023

Revised: 13 March 2023

Accepted: 16 March 2023

Published: 20 March 2023



Copyright: © 2023 by the authors. Licensee MDPI, Basel, Switzerland. This article is an open access article distributed under the terms and conditions of the Creative Commons Attribution (CC BY) license (<https://creativecommons.org/licenses/by/4.0/>).

1. Introduction

The real-time synchronisation of loads and demands is essential for the steady operation of a power system. The LFC technology is used to accomplish this objective. One of the most fundamental issues in managing power systems involves monitoring the frequency to detect any mismatch between the power generation and load. The three primary functions of the LFC system are to maintain a steady frequency, distribute the load among the generators, and manage the schedule for tie-line interchanges [1]. In an LFC system, a communication channel (i.e., between plant and controller) is typically utilised in the feedback loop to transmit and receive signals or information that are used to exercise control, which introduces temporal delays into the feedback path [2]. The delay is unavoidable, particularly if the power system adopts open communications [3]. Furthermore, this affects the performance of the LFC systems, which can cause instability [4,5]. Therefore, a less

conservative and accurate delay-dependent stability analysis procedure must be used to compute a maximum DM for the LFC systems for various subsets of controller parameters so that it can be used as a practical guideline for fine-tuning controller parameters during implementation, even with only partial knowledge of network delays.

Several studies have recently been conducted to alleviate the issue of temporal delays in LFC systems. The current state-of-the-art in the literature to determine the DM of the LFC systems are namely the frequency-domain and the time-domain methods. In the frequency domain, the time delay of a system can be identified by determining the crossing frequency of a system, where the roots cross the imaginary axis. Meanwhile, in the time domain, the Lyapunov–Krasovskii functional (LKF) is employed to derive the stability condition in the form of a linear matrix inequality (LMIs).

The computational DM specifically for a constant time delay for LFC was developed by many researchers which will be discussed as follows. In [6], LKF is employed with truncated second-order Bessel–Legendre (BL) inequality to restrict the time derivatives of the states for the single-area and multi-area LFC systems with a PI controller. The stability margin is calculated using LMIs, where a binary search iteration algorithm is used to accurately determine the DM. In [7], the DM was examined by the generalised modified Mikhailov criterion in the time domain for a single-area LFC system with fractional order PI controller. The DM is obtained by solving the fractional polynomial equation and determining the intersection at the imaginary axis. In [8], the BL inequality and LKF are utilised to approximate the functional derivative and determine the largest possible lower bound for the LFC system that incorporates a PID controller. The time delay stability margin is solved using the MATLAB LMI toolbox. In [9], a novel augmented Lyapunov functional is constructed with the lower order and the derivative is bounded with the Wirtinger inequality for multi-area LFC schemes. In [10], LKF is employed with quadratic generalised free-weighting matrix inequality to tighten the boundary of the time derivatives for a single-area LFC system. In [11], LKF is employed with single- and double-integral terms for accurate integral inequalities and a new nonlinear optimisation technology was employed to solve the problem of nonlinear time-delay inequalities. In [12], LKF is employed with a triple integral term and using the method of integral inequality for one area and two area LFC. In [13], a modified LKF with delay-dependent matrices containing single-integral items and a unique negative definite inequality equivalent transformation lemma is utilised to translate the nonlinear inequality into LMIs for one and two-area LFC systems. In [14], a novel LKF is employed with quadratic terms multiplied by first, second, and third degrees of scalar functions for one and two-area LFC systems with the PI controller. In [15], a modified LKF is employed, involving the delay-dependent non-integral items and some augmented single-integral items for a single-area power system. In [16], the computation of DM is determined by converting the transcendental equation into nonlinear equations by introducing a new variable. It is reported that the results are more accurate, where the crossing frequency is determined by implementing the sweeping test. It has been shown in prior work that the LFC system has a time delay, and that computing it is crucial for practical purposes due to the majority of existing approaches having advanced complex mathematical analysis and involving numerous computations to determine the DM; however, engineers require a method that is quick and precise in practice [17].

A precise frequency domain technique for DM calculation is described in [18], where the stability condition is constructed and the characteristic equation is translated into a polynomial equation. Exact DM values are acquired by precisely determining the crossing frequencies. The sweeping test in [16,19] determines the precise values of the DM, however, the test is highly dependent on the sweeping range and the sweeping step size. It must be noted that employing the sweeping test with high accuracy (i.e., very small step size) can be time-consuming. Furthermore, the majority of researchers are focused on building a new algorithm for determining the exact DM through the iteration process. However, there is not much effort made to combine optimisation approaches with the existing DM algorithms. This study aimed to eliminate the iteration process and to determine the more

accurate results of DM by introducing an optimisation technique. It is expected that by combining an optimisation technique with the existing DM algorithm, the DM results for a constant time delay problem will be more accurate and reliable. Furthermore, it has been proven in [20–27] that the combination of a metaheuristic optimisation technique and a conventional algorithm provides a significant improvement in many power system applications and other real-world problems.

In this paper, the method of improving the computation of the DM using GWO for a constant time delay is presented. The proposed method is developed to optimise the minimum error and thus, determine the best design variable (i.e., the crossing frequency). The crossing frequency obtained from the proposed method will lead to an accurate result of the DM. Furthermore, the contribution of this paper is that the proposed method can address the problem, as mentioned in [17], where the proposed method does not require any sweeping range, sweeping step size, or iteration method to determine the accurate crossing frequency. In addition, an objective function is introduced and formulated using the existing theorem to determine the optimal crossing frequency with minimal error. The proposed method is realised in a two-area network power system, and the DM values are compared with the methods in [18,28] for the different values of K_P and K_I . It is observed during the simulation that the DM results are more accurate and stable compared to [18,19,28,29]. The simulation was run for a prolonged period of time to avoid inaccuracy in the results. The remainder of the article is organised as follows: The dynamic model of a two-area LFC system with time delay is defined in Section 2, the overview of GWO is detailed in Section 3, the proposed computation of DM based on GWO is described in Section 4, the results are discussed in Section 5, and this article is concluded in Section 6.

2. Dynamic Model of Two-Area LFC System with Time Delay

Figure 1 depicts a standard model of a two-area LFC system. The network is made up of a governor, a turbine, a rotating mass, a PI controller, communication delay, and a load with the feedback of regulation constant and area control error (i.e., ACE_1 and ACE_2) for both areas (i.e., area 1 and area 2). The disturbance in the system happens when the load changes, as indicated by ΔP_{d1} and ΔP_{d2} . When the load on the system increases, the turbine speed decreases until the governor can adjust the steam input into the new load. The error signal decreases as the variation in speed value decreases, and the governor setting approaches the point required to keep the speed constant.

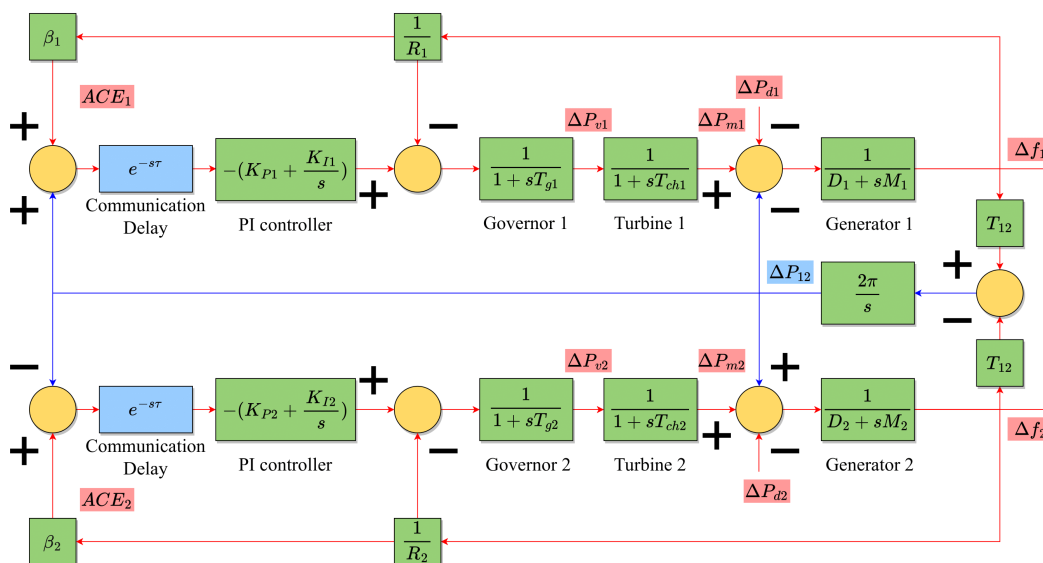


Figure 1. Two-area LFC scheme [28,30].

In terms of its state-space model, the model of Figure 1 with communication delay is defined as [28,30]:

$$\dot{x}(t) = Kx(t) + K_d x(t - \tau) + F \Delta P_d \tag{1}$$

$$x(t) = [\Delta f_1(t) \quad \Delta P_{m1}(t) \quad \Delta P_{v1}(t) \quad \int ACE_1 dt \quad \Delta P_{12}(t) \quad \Delta f_2(t) \quad \Delta P_{m2}(t) \quad \Delta P_{v2}(t) \quad \int ACE_2 dt]^T \tag{2}$$

$$K = \begin{bmatrix} -\frac{D_1}{M_1} & \frac{1}{M_1} & 0 & 0 & -\frac{1}{M_1} & 0 & 0 & 0 & 0 \\ 0 & -\frac{1}{T_{ch1}} & \frac{1}{T_{ch1}} & 0 & 0 & 0 & 0 & 0 & 0 \\ -\frac{1}{R_1 T_{g1}} & 0 & -\frac{1}{T_{g1}} & 0 & 0 & 0 & 0 & 0 & 0 \\ \beta_1 & 0 & 0 & 0 & 1 & 0 & 0 & 0 & 0 \\ 2\pi T_{12} & 0 & 0 & 0 & 0 & -2\pi T_{12} & 0 & 0 & 0 \\ 0 & 0 & 0 & 0 & \frac{1}{M_2} & -\frac{D_2}{M_2} & \frac{1}{M_2} & 0 & 0 \\ 0 & 0 & 0 & 0 & 0 & 0 & -\frac{1}{T_{ch2}} & \frac{1}{T_{ch2}} & 0 \\ 0 & 0 & 0 & 0 & 0 & -\frac{1}{R_2 T_{g2}} & 0 & -\frac{1}{T_{g2}} & 0 \\ 0 & 0 & 0 & 0 & -1 & \beta_2 & 0 & 0 & 0 \end{bmatrix} \tag{3}$$

$$K_d = \begin{bmatrix} 0 & 0 & 0 & 0 & 0 & 0 & 0 & 0 & 0 \\ 0 & 0 & 0 & 0 & 0 & 0 & 0 & 0 & 0 \\ -\frac{\beta_1 K_{P1}}{T_{g1}} & 0 & 0 & -\frac{K_{I1}}{T_{g1}} & -\frac{K_{P1}}{T_{g1}} & 0 & 0 & 0 & 0 \\ 0 & 0 & 0 & 0 & 0 & 0 & 0 & 0 & 0 \\ 0 & 0 & 0 & 0 & 0 & 0 & 0 & 0 & 0 \\ 0 & 0 & 0 & 0 & 0 & 0 & 0 & 0 & 0 \\ 0 & 0 & 0 & 0 & 0 & 0 & 0 & 0 & 0 \\ 0 & 0 & 0 & 0 & \frac{K_{P2}}{T_{g2}} & -\frac{\beta_2 K_{P2}}{T_{g2}} & 0 & 0 & -\frac{K_{I2}}{T_{g2}} \\ 0 & 0 & 0 & 0 & 0 & 0 & 0 & 0 & 0 \end{bmatrix} \tag{4}$$

$$F = \begin{bmatrix} -\frac{1}{M_1} & 0 & 0 & 0 & 0 & 0 & 0 & 0 & 0 \\ 0 & 0 & 0 & 0 & 0 & -\frac{1}{M_2} & 0 & 0 & 0 \end{bmatrix}^T \tag{5}$$

where Δf_1 and Δf_2 are the frequency deviations in area 1 and area 2, ΔP_{m1} and ΔP_{m2} are the mechanical output power deviation in area 1 and area 2, ΔP_{v1} and ΔP_{v2} are the valve position deviation in area 1 and area 2, ΔP_{12} is the power transfer deviation in tie-line between the two areas, D_1 and D_2 are the generator damping coefficient in area 1 and area 2, M_1 and M_2 are the moment of inertia of generator in area 1 and area 2, T_{ch1} and T_{ch2} are the turbine time constant in area 1 and area 2, T_{g1} and T_{g2} are the governor time constant in area 1 and area 2, R_1 and R_2 are the speed drop in area 1 and area 2, β_1 and β_2 are the frequency bias factor in area 1 and area 2, T_{12} is the synchronising coefficient of the tie-line between two areas, K_{p1} and K_{p2} are the proportional gain of the PI controller in area 1 and area 2, and K_{i1} and K_{i2} are the integral gain of the PI controller in area 1 and area 2. The area control error, ACE, is calculated for each control region as the sum or difference of the power transfer along the tie-line connecting the two areas and scaled by a frequency bias factor, which can be defined as [18,29]:

$$ACE_1(t) = \beta_1 \Delta f_1(t) + \Delta P_{12}(t) \quad (6)$$

$$ACE_2(t) = \beta_2 \Delta f_2(t) - \Delta P_{12}(t) \quad (7)$$

The time delay τ is made up of the following components: the transducer delay, the delay in the communication connection, the delay in processing, the delay in multiplexing, and the delay in the analogue-to-digital conversion [31]. In dedicated communication channels, this delay is constant, but if open communication is utilised, it may fluctuate in length [29]. The two-area LFC system becomes a linear time delay system when ΔP_d is set to zero, Equation (1) may then be stated as follows [16]:

$$\dot{x}(t) = Kx(t) + K_d x(t - \tau) \quad (8)$$

The maximum DM, τ_d , can be determined by transforming Equation (8) into the s-domain using the Laplace transform and can be expressed as:

$$sI - K - K_d e^{-s\tau} = 0 \quad (9)$$

The system is asymptotically stable for the given delay [16], if all of the roots of Equation (9) are situated on the left half plane. All of the roots of the free delay system are on the left half plane, and it is assumed the system is stable. In this paper, the frequency domain approach is employed to determine the maximum time delay using grey wolf optimisation, which will be discussed in the next section.

3. Overview of Grey Wolf Optimisation

A pack of grey wolves surrounding and assaulting prey for food is a simplistic depiction of the grey wolf optimisation algorithm, in which they have a disciplined social dominating hierarchy beginning with alpha, beta, delta, and omega [32]. Grey wolves' hunting behaviour may be separated into three stages, namely the tracking, surrounding, and attacking prey. To begin, surrounding the prey may be defined as [32,33]:

$$\vec{D}\vec{V} = |\vec{C}\vec{V} \cdot \vec{X}\vec{V}_p(t) - \vec{X}\vec{V}(t)| \quad (10)$$

$$\vec{X}\vec{V}(t+1) = \vec{X}\vec{V}_p(t) - \vec{A}\vec{V} \cdot \vec{D}\vec{V} \quad (11)$$

where t denotes the iteration, $\vec{X}\vec{V}_p$ is the position vector of the prey, $\vec{X}\vec{V}$ is the position vector of a grey wolf, $\vec{A}\vec{V}$ and $\vec{C}\vec{V}$ are the coefficient vectors, and $\vec{D}\vec{V}$ is the distance between the position vectors of the prey and a grey wolf. These coefficients can be calculated by:

$$\vec{A}\vec{V} = 2\vec{b} \cdot \vec{r}_1 - \vec{b} \quad (12)$$

$$\vec{C}\vec{V} = 2 \cdot \vec{r}_2 \quad (13)$$

where \vec{b} decreases linearly over the length of iterations from 2 to 0 and \vec{r}_1, \vec{r}_2 are random vectors in $[0, 1]$. Meanwhile, grey wolf hunting behaviour may be analytically described as [32,33]:

$$\vec{XV}_1 = \vec{XV}_\alpha - \vec{AV}_1 \cdot (D\vec{V}_\alpha) \quad (14)$$

$$\vec{XV}_2 = \vec{XV}_\beta - \vec{AV}_2 \cdot (D\vec{V}_\beta) \quad (15)$$

$$\vec{XV}_3 = \vec{XV}_\delta - \vec{AV}_3 \cdot (D\vec{V}_\delta) \quad (16)$$

$$\vec{XV}(t+1) = \frac{\vec{XV}_1 + \vec{XV}_2 + \vec{XV}_3}{3} \quad (17)$$

where subscript α indicates the best candidate for searching the prey. Meanwhile, the subscripts β and δ represent the second and third best solution, respectively.

4. Delay Margin Computation Based on Grey Wolf Optimisation

As discussed in Reference [16], systems that deal with time delays can either be delay-dependent or delay-independent. A delay-independent system is said to be asymptotically stable only if the value of time delay is positive. However, in a delay-dependent system, the system is said to be asymptotically stable, marginally stable, and asymptotically unstable, if the value of $\tau < \tau_d$, $\tau = \tau_d$, and $\tau > \tau_d$, respectively. The LFC system modelled in Equation (8) is said to be asymptotically stable independent of delay if it satisfies the condition stipulated in [34], as described in Equations (18) and (19):

$$\det(j\omega I - K - K_d e^{-j\omega\tau}) \neq 0, \forall \omega > 0, \forall \tau \in [0, \infty) \quad (18)$$

$$\lim_{\omega \rightarrow \infty} \rho((j\omega I - K)^{-1} K_d) = 0 \quad (19)$$

If Equations (18) and (19) are satisfied, this means that the system does not intersect the imaginary axis. However, the system is said to be delay-dependent stable, if Equations (18) and (19) do not meet for some values of ω . Where for $\tau < \tau_d$, all roots lie on the closed left half plane, for $\tau > \tau_d$, some roots will lie on the right plane, and for $\tau = \tau_d$, the roots will intersect with the imaginary axis. The following definition, as explained in Reference [16], uses the spectral radius to determine the crossover frequency, ω_c , at which the roots cross the imaginary axis.

Definition 1 ([34]). *A pair of matrices' combined spectral radius can be described as:*

$$\underline{\rho}(K, K_d) := \min\{|\lambda| \mid \det(K - \lambda K_d) = 0\} \quad (20)$$

where $\lambda_i(K)$ and $\lambda_i(K, K_d)$ are the i th eigenvalue of the matrix K and the generalised eigenvalue of matrix pair K and K_d , respectively.

To determine the maximum DM, we use the sweeping test [34] in the ω domain. The sweeping test is a very useful technique, especially in light of the improvements in computational power seen in modern computers. The sweeping test is superior since it requires less computation and produces accurate results. We apply the following theorem to determine the DM of the two-area LFC system.

Theorem 1 ([34]). *We can define a stable system (8) at $\tau_d = 0$, where $K + K_d$ is stable and $\text{rank}(K_d) = q$.*

$$\bar{\tau}_i := \begin{cases} \min_{1 \leq k \leq n} \frac{\theta_k^i}{\omega_k^i}, & \text{if } \lambda_i(j\omega_k^i I - K, K_d) = e^{-j\theta_k^i} \\ \infty, & \text{for some } \omega_k^i \in (0, \infty), \theta_k^i \in [0, 2\pi] \\ & \underline{\rho}(j\omega I - K, K_d) > 1 \forall \omega \in (0, \infty) \end{cases} \quad (21)$$

Then,

$$\bar{\tau}_d := \min_{1 \leq i \leq q} \bar{\tau}_i$$

where the system in (8) is unstable at $\tau = \tau_d$ and stable for all $\tau \in [0, \infty)$.

Proof ([34–37]). The system (8) is considered stable for any time delay when Equation (22) is satisfied:

$$\underline{\rho}(j\omega I - K, K_d) = \underline{\rho}(j\omega I - K, K_d e^{-j\omega\tau}) > 1, \text{ for } \omega > 0, \tau \geq 0 \quad (22)$$

According to the condition of Equation (22), the system is stable when $\tau = 0$, $\det(K + K_d) \neq 0$, and $\omega = 0$. However, it is unstable for a certain τ for $\tau_d < \infty$. Then, the following assumption is examined:

$$\det(j\omega I - K - K_d e^{-j\omega\tau}) \neq 0, \forall \omega \in [0, \infty) \quad (23)$$

This is true for $\omega \neq \omega_k^i$, or else:

$$|\lambda_i(j\omega I - K, K_d)| \neq 1, i = 1, 2, 3, \dots, m \quad (24)$$

For $\tau \in [0, \tau_d)$, $\tau\omega_k^i \neq \theta_k^i$, Equation (25) is satisfied:

$$\det(j\omega_k^i I - K - K_d e^{-j\omega_k^i\tau}) \neq 0 \quad (25)$$

Equation (26) is satisfied if $\tau = \tau_d$, such that (ω_k^i, θ_k^i) is unique, which satisfies $\tau_d = \theta_k^i / \omega_k^i$, and consequently:

$$\det(j\omega_k^i I - K - K_d e^{-j\omega_k^i\tau_d}) = \det(j\omega_k^i I - K - K_d e^{-j\theta_k^i\tau_d}) = 0 \quad (26)$$

□

Corollary 1 ([34]). *If and only if the system (8) is stable regardless of delay:*

- K is stable;
- $K + K_d$ is stable, and;
- $\underline{\rho}(j\omega I - K, K_d) > 1, \forall \omega > 0$.

The delay-independent stability is represented by the three conditions in Corollary 1, where the first and second conditions state that the system is stable for $\tau = 0$ and $\tau = \infty$, respectively. The third condition states that the system is stable for $\tau \in [0, \infty)$. Finally, we can compute the exact DM by using Theorem 1 to determine the system stability (i.e., delay-independent or delay-dependent stability). First, we can examine the condition in Equation (22) to see if the system (8) is delay independent. For some values of ω , if Equation (22) is not satisfied, the crossing frequency is determined using the proposed algorithm in Figure 2.

To begin, the system matrices for a two-area network are calculated using Equations (3) and (4). This is followed by the objective function to minimise the error of the spectral radius, ϵ , and can be expressed as:

$$f = \min(\epsilon) \quad (27)$$

$$\epsilon = |1 - \underline{\rho}(j\omega I - K, K_d)| \quad (28)$$

where integer 1 is the desired spectral radius at the crossing frequency, ω_c . Furthermore, ω , is the only decision variable in this problem. The constraint can be expressed as:

$$0 \leq \omega \leq \omega_{max} \quad (29)$$

where ω_{max} is the maximum frequency desired by the user. Once the GWO algorithm found the optimal solution in the search space, the best design variable ω is then updated to determine the value of the crossing angle, θ , which can be expressed as:

$$\lambda_i(j\omega I - K, K_d) = e^{-j\theta} \quad (30)$$

Finally, the desired DM is calculated as:

$$\tau_d = \min_{1 \leq k \leq n} \frac{\theta_k^i}{\omega_k^i} \quad (31)$$

In the event that the algorithm is unable to identify the optimum solution, the decision variable is randomly re-initialised in an effort to locate the optimal solution in the search space.

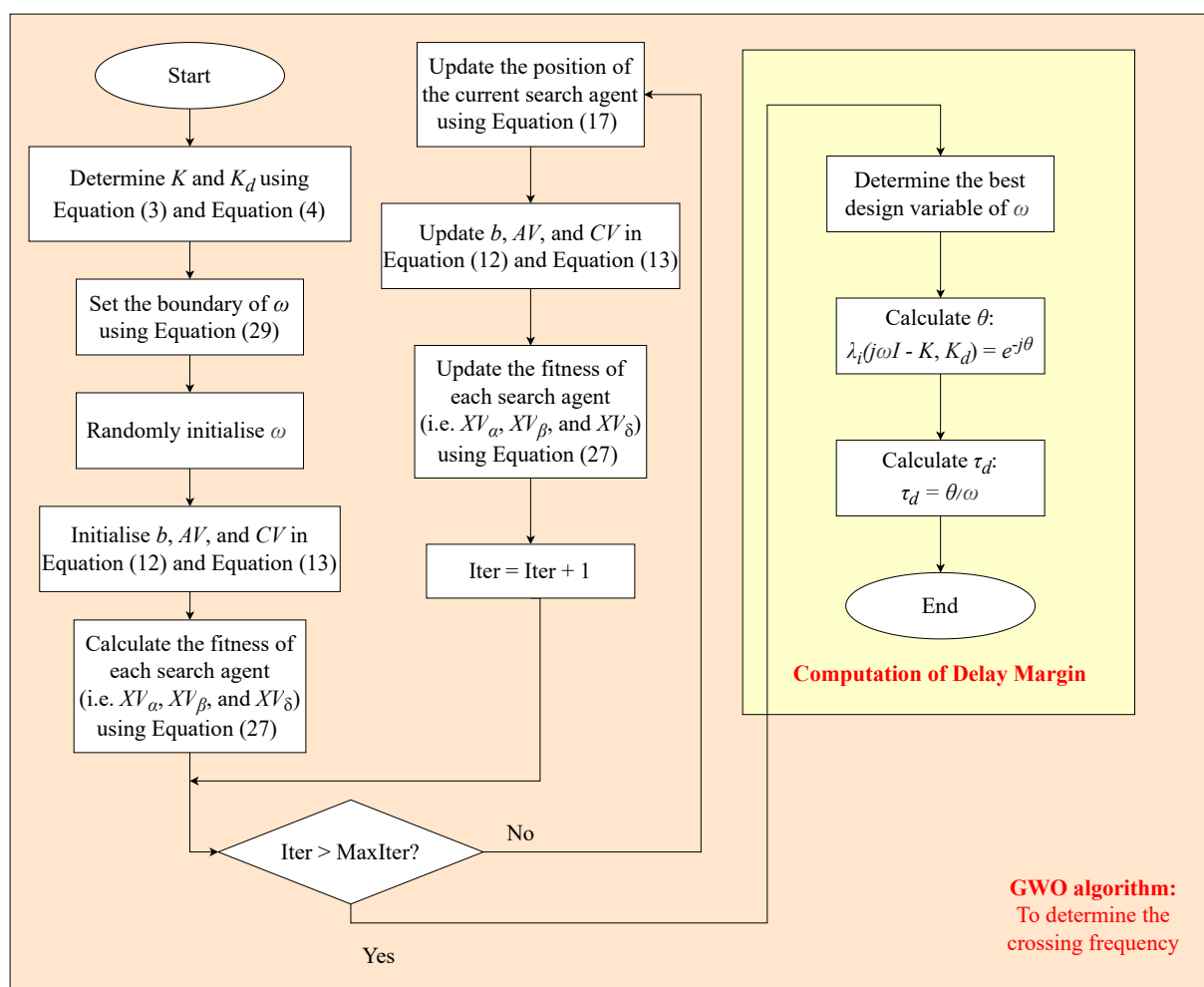


Figure 2. Flowchart of the proposed DM computation based on GWO.

5. Case Study: Two-Area LFC System

Three case studies for a two-area LFC system are presented in this section. We utilise the parameters in References [18,28,29] to compare the outcomes of our suggested approach with those that have already been published. Table 1 tabulates the system DM for various PI controller gains, K_P and K_I , as well as the results of the methods in references [18,19,28,29]. It is noteworthy that the approach described in reference [18] offers the highest degree of accuracy-reported DMs. Moreover, the GWO algorithm has a maximum population size and maximum iterations of 50 and 200, respectively.

Table 1. The DM for various K_P and K_I values.

K_P	τ_d, s				K_I			
	Method	0.05	0.10	0.15	0.20	0.40	0.60	1.0
0.0	Proposed method	30.935	15.200	9.949	7.322	3.235	1.851	0.586
	[18]	30.812	15.090	9.842	7.211	3.225	1.843	0.591
	[19]	30.827	15.178	-	7.225	3.275	1.930	-
	[28]	30.756	15.072	9.835	7.210	3.231	1.849	0.586
	[29]	27.848	13.699	8.974	6.603	3.002	1.745	0.573
0.05	Proposed method	31.895	15.680	10.269	7.561	3.354	1.930	0.631
	[18]	31.772	15.570	10.162	7.450	3.345	1.922	0.638
	[19]	31.763	15.587	-	7.509	3.399	2.008	-
	[28]	31.704	15.547	10.152	7.448	3.350	1.928	0.631
	[29]	27.830	14.020	9.205	6.777	3.095	1.810	0.616
0.10	Proposed method	32.772	16.117	10.560	7.780	3.462	2.000	0.669
	[18]	32.647	16.008	10.453	7.669	3.453	1.993	0.676
	[19]	32.632	16.021	-	7.700	3.507	2.079	-
	[28]	31.083	15.968	10.440	7.664	3.457	1.998	0.669
	[29]	27.001	13.650	9.166	6.881	3.174	1.863	0.649
0.20	Proposed method	34.248	16.852	11.050	8.146	3.641	2.113	0.716
	[18]	34.122	16.744	10.943	8.035	3.631	2.106	0.725
	[19]	34.1563	16.768	-	8.058	3.694	2.1975	-
	[28]	28.579	15.102	10.495	7.998	3.634	2.110	0.716
	[29]	25.090	12.702	8.572	6.497	3.209	1.931	0.692
0.40	Proposed method	35.845	17.647	11.574	8.536	3.812	2.189	0.662
	[18]	35.728	17.542	11.469	8.424	3.802	2.184	0.684
	[19]	35.7223	17.566	-	8.4673	3.876	2.2997	-
	[28]	22.841	12.196	8.609	6.781	3.778	2.184	0.662
	[29]	20.278	10.364	7.014	5.338	2.735	1.731	0.637
0.60	Proposed method	34.914	17.162	11.239	8.275	3.597	1.874	0.454
	[18]	34.809	17.068	11.136	8.155	3.588	1.881	0.480
	[19]	34.8393	17.103	-	8.2113	3.710	2.1141	-
	[28]	16.254	8.839	6.387	5.134	3.089	1.864	0.454
	[29]	14.228	7.332	4.944	3.768	1.920	1.198	0.443
1.0	Proposed method	0.555	0.546	0.537	0.526	0.482	0.434	0.339
	[18]	0.510	0.498	0.485	0.472	0.416	0.357	0.243
	[19]	-	-	-	-	-	-	-
	[28]	0.486	0.474	0.462	0.450	0.396	0.339	0.229
	[29]	0.465	0.455	0.444	0.433	0.384	0.332	0.227

- Data are not available from the published paper.

Table 1 shows that the proposed method yields remarkably similar results to the method described in Reference [18]. Furthermore, the proposed method provides fewer computations by reducing the mathematical complexity to obtain the system DMs. Figures 3–9 compare the proposed method to the methods given in References [18,28]. For various values of proportional gain, K_P , they show the DM, τ_d , versus the integral gain, K_I , curve. It is obvious that the proposed method precisely and accurately calculates the DM for the two-area LFC system for a variety of K_I and K_P values. Furthermore, the relative inaccuracy of the suggested approach and the one stated in [18] is rather minor. More importantly, the average relative percentage error is only 3.1611%, and thus, demonstrates that the DM values are nearly identical to those provided in [18].

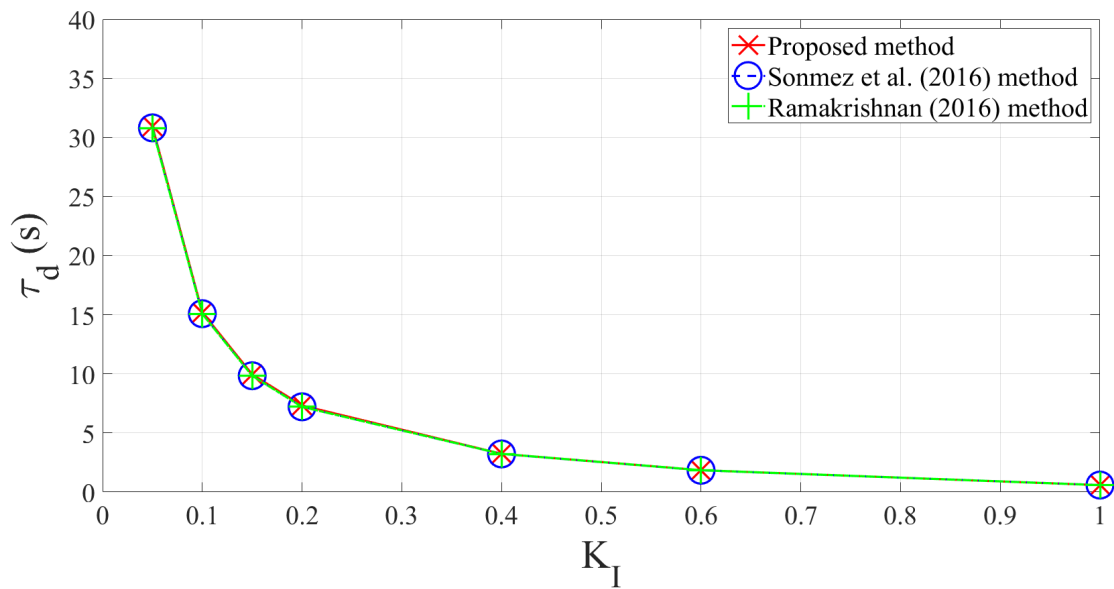


Figure 3. With $K_P = 0$, the DM, τ_d , is shown against the integral gain, K_I , curve [18,28].

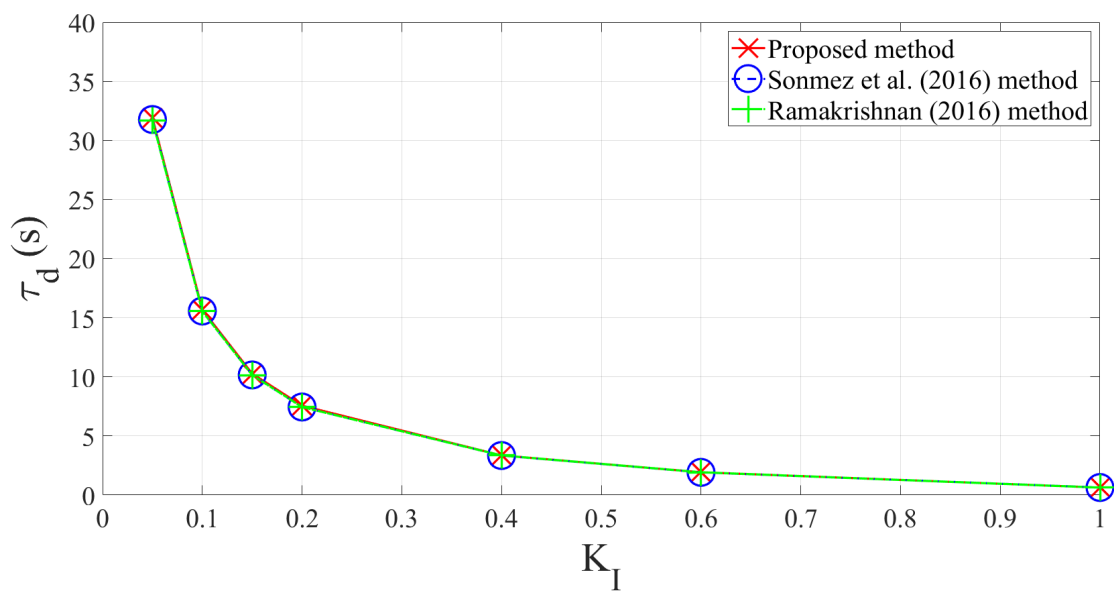


Figure 4. With $K_P = 0.05$, the DM, τ_d , is shown against the integral gain, K_I , curve [18,28].

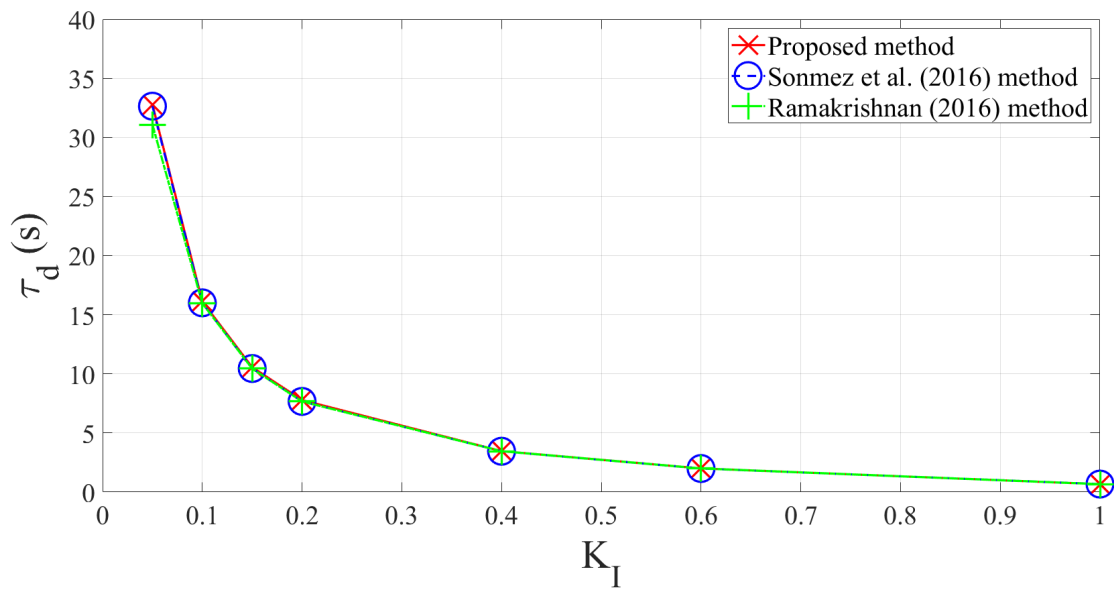


Figure 5. With $K_p = 0.1$, the DM, τ_d , is shown against the integral gain, K_I , curve [18,28].

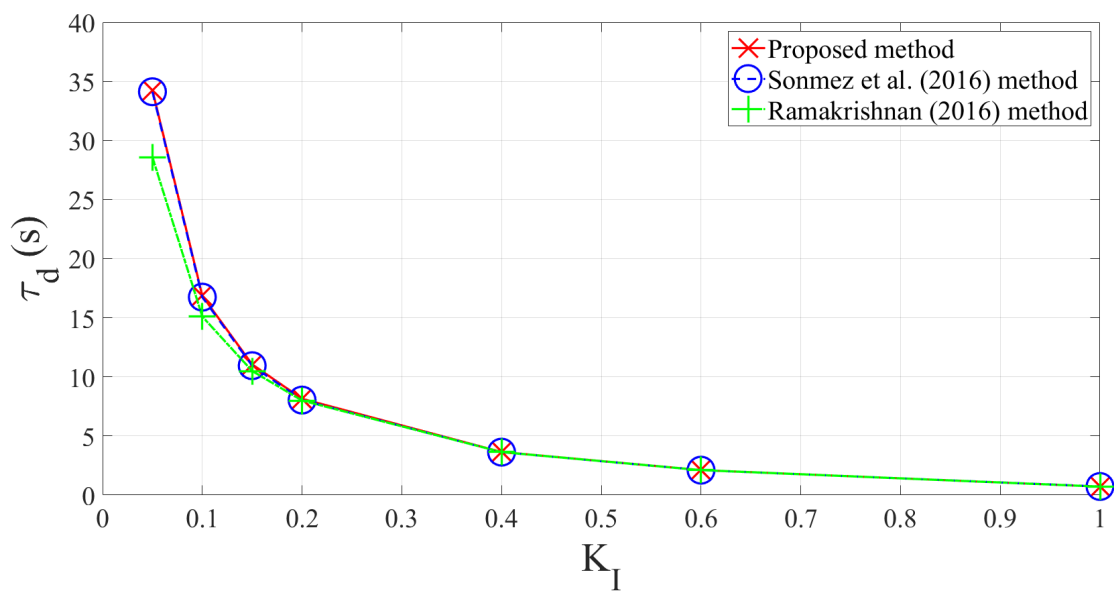


Figure 6. With $K_p = 0.2$, the DM, τ_d , is shown against the integral gain, K_I , curve [18,28].

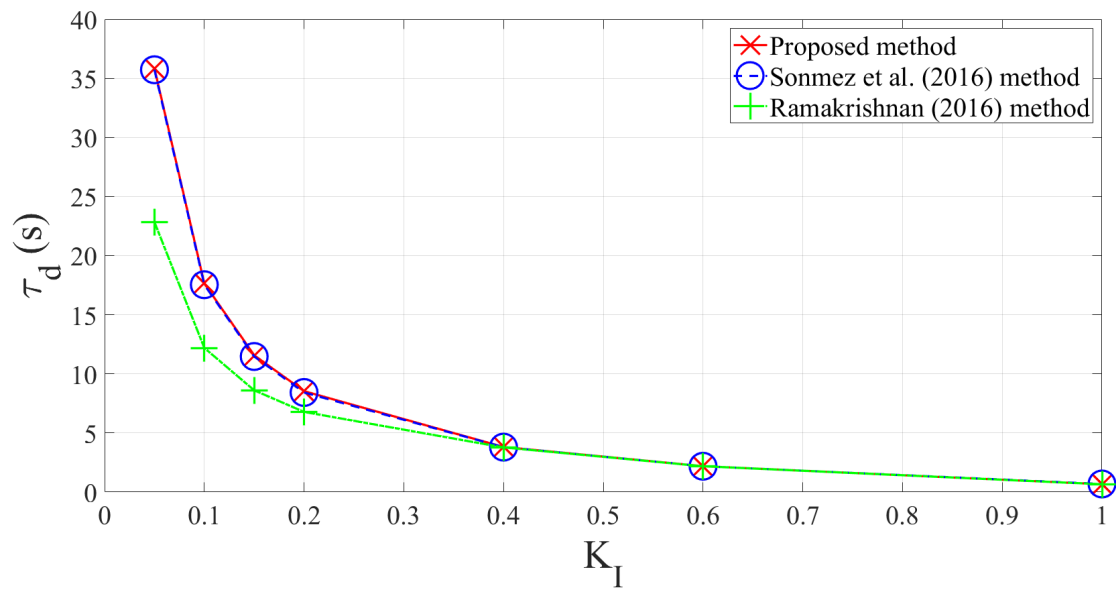


Figure 7. With $K_p = 0.4$, the DM, τ_d , is shown against the integral gain, K_I , curve [18,28].

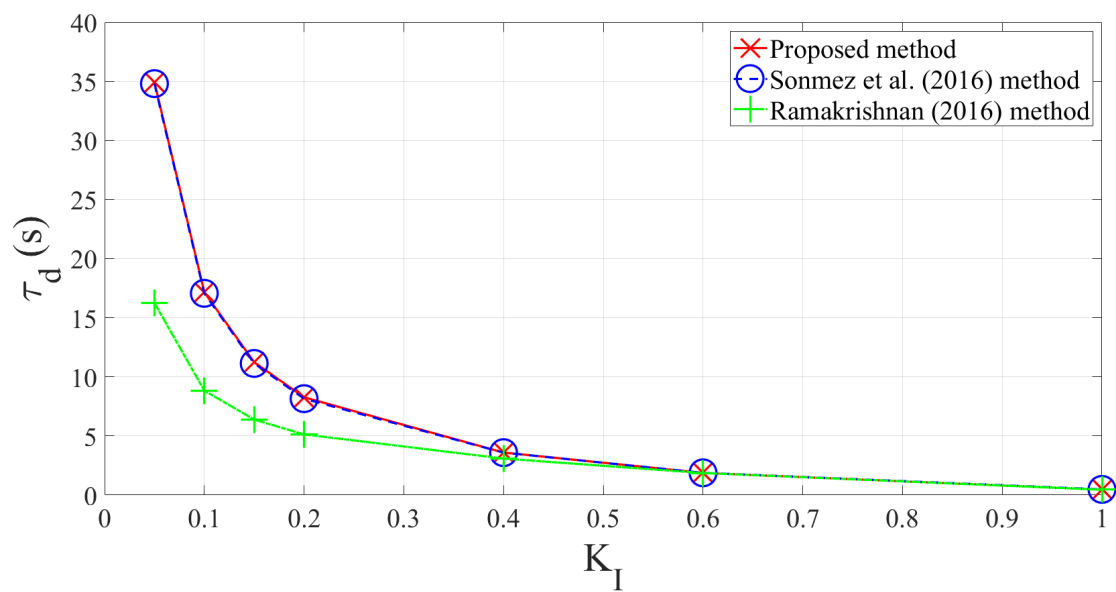


Figure 8. With $K_p = 0.6$, the DM, τ_d , is shown against the integral gain, K_I , curve [18,28].

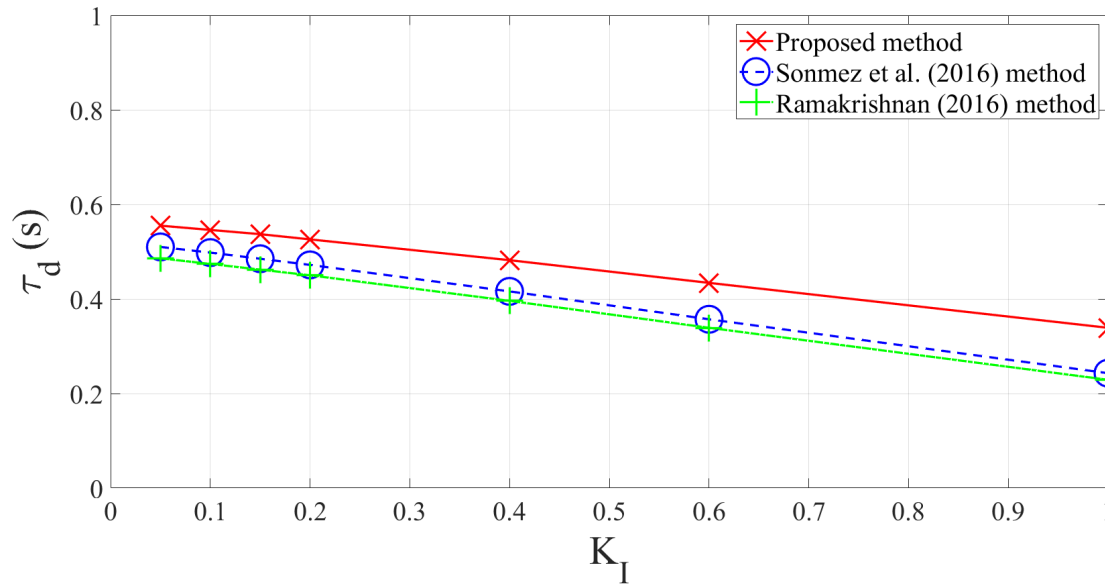


Figure 9. With $K_P = 1.0$, the DM, τ_d , is shown against the integral gain, K_I , curve [18,28].

Case study 1 with $K_P = 0.2$ and $K_I = 0.4$: The DM estimated using the method provided in [18] is 3.631 s, while it was 3.641 s with the proposed method. The proposed method, just like the method described in [18], gives precise DM values. Simulations with Matlab/Simulink are performed to validate the results. Figures 10 and 11 showcase the frequency response of a two-area LFC system when subjected to different time delay values in area 1 and area 2, while utilising $K_P = 0.2$ and $K_I = 0.4$. At 10 s, the load changes, ($\Delta P_{d1} = \Delta P_{d2}$), by 0.1 p.u. Figures 10 and 11 depict the frequency response with time delay, τ , of 3.5 s, 3.641 s, and 3.7 s, for area 1 and area 2, respectively. It is obvious that the system is stable with $\tau = 3.5$ s and unstable with $\tau = 3.7$ s. Meanwhile, the system is marginally stable with $\tau = 3.641$ s.

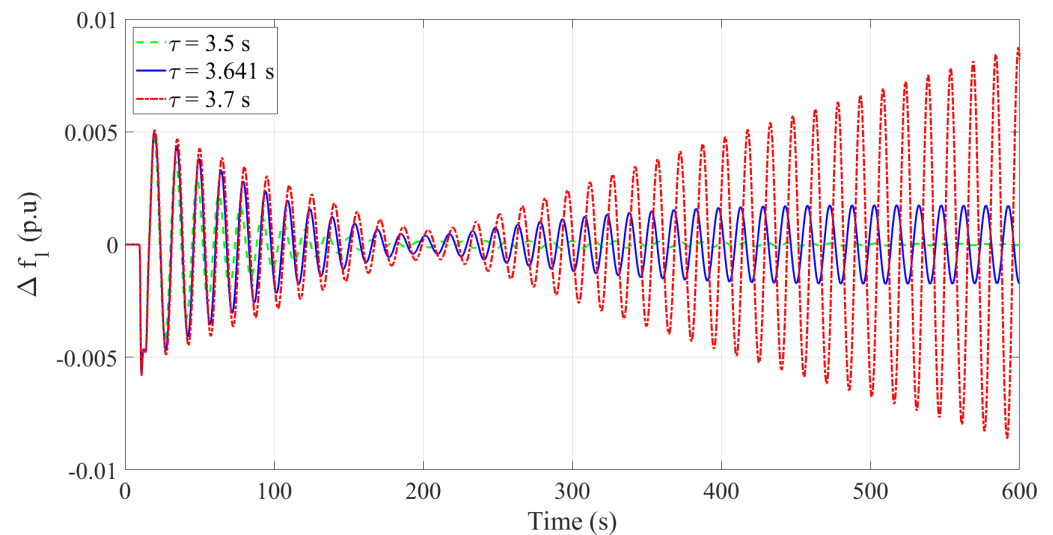


Figure 10. Frequency deviation for LFC-1: Δf_1 was measured while using $K_P = 0.2$ and $K_I = 0.4$.

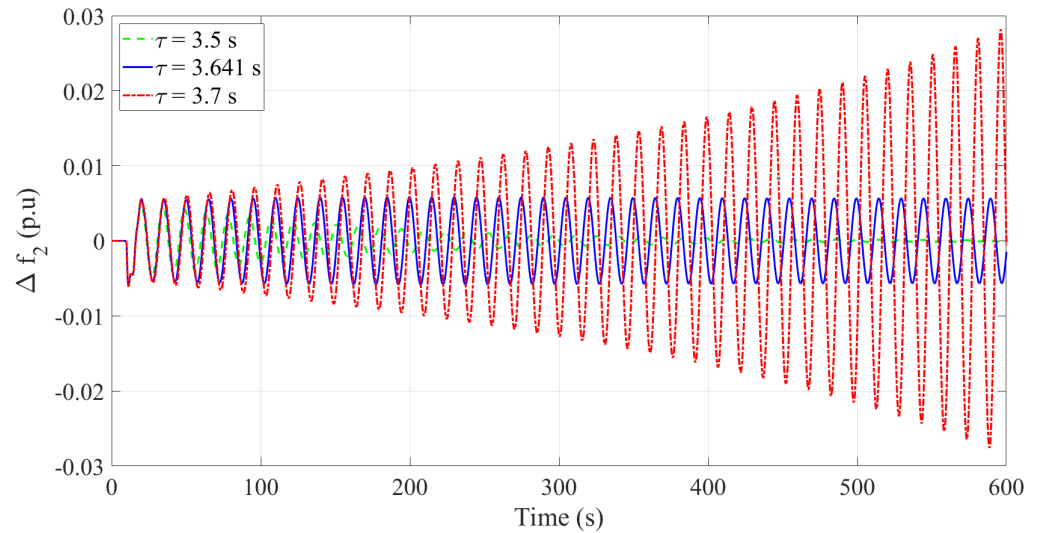


Figure 11. Frequency deviation for LFC–2: Δf_2 , was measured while using $K_P = 0.2$ and $K_I = 0.4$.

The percentage inaccuracy while employing the simulation-based DM is 0.000%. Figure 12 depicts the spectral radius against the frequency for $K_P = 0.2$ and $K_I = 0.4$. It was found that the crossing frequency, ω_c , was equal to 0.41914 rad/s with $\theta = 1.5261$ rad. By solving Equation (31), we obtain the DM equal to 3.641 s.

Case study 2 with $K_P = 0.4$ and $K_I = 0.6$: The DM estimated using the method provided in [18] is 2.184 s, while it was 2.189 s with the proposed method. The frequency response of the two-area LFC system was illustrated in Figures 13 and 14, taking into account the impact of various time delays on area 1 and area 2, while setting $K_P = 0.4$ and $K_I = 0.6$.

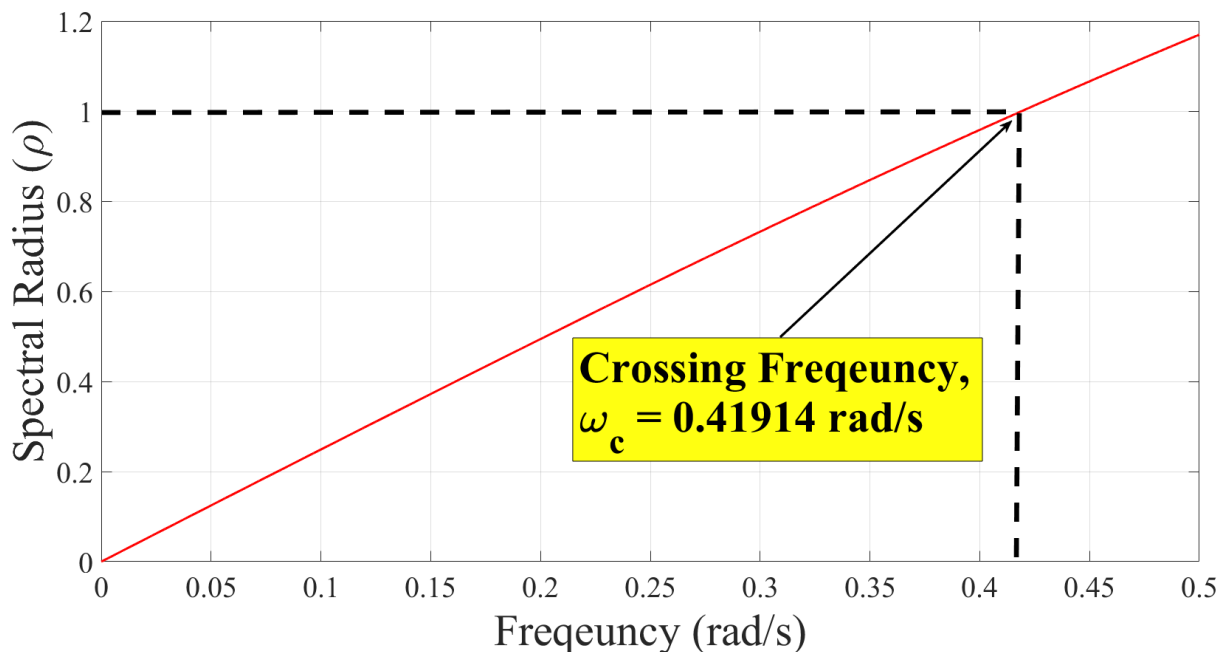


Figure 12. The spectral radius, ρ , against the frequency, ω , for $K_P = 0.2$ and $K_I = 0.4$.

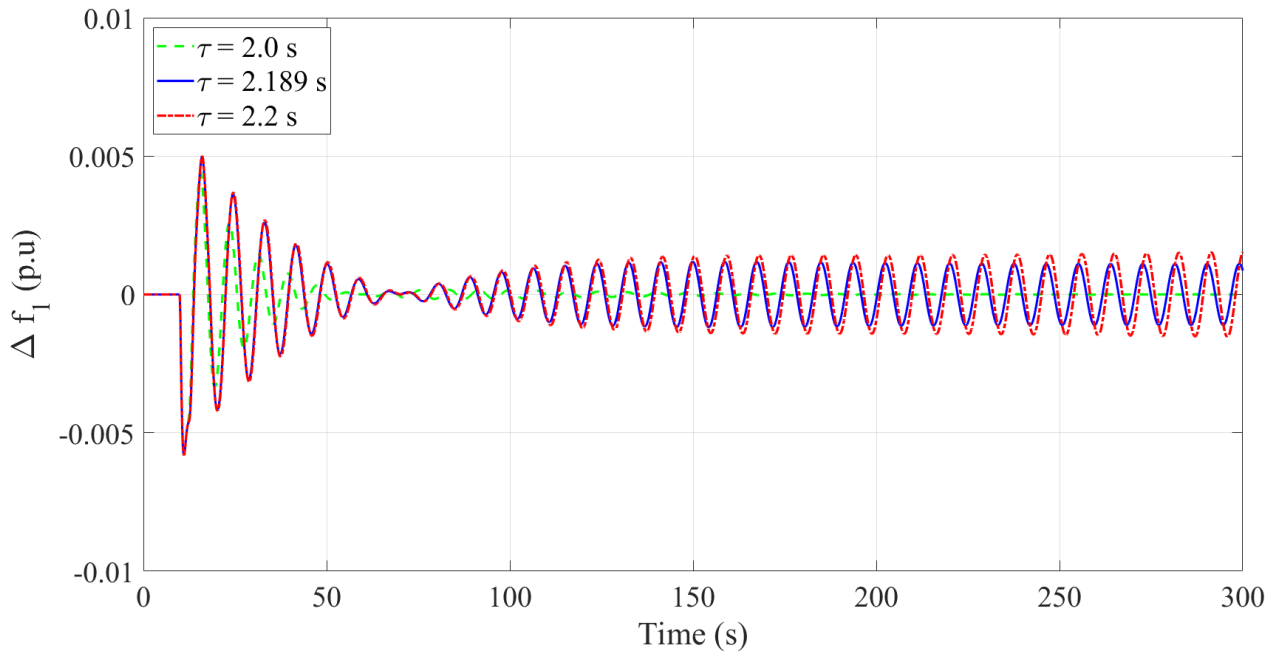


Figure 13. Frequency deviation for LFC-1: Δf_1 was measured while using $K_P = 0.4$ and $K_I = 0.6$.

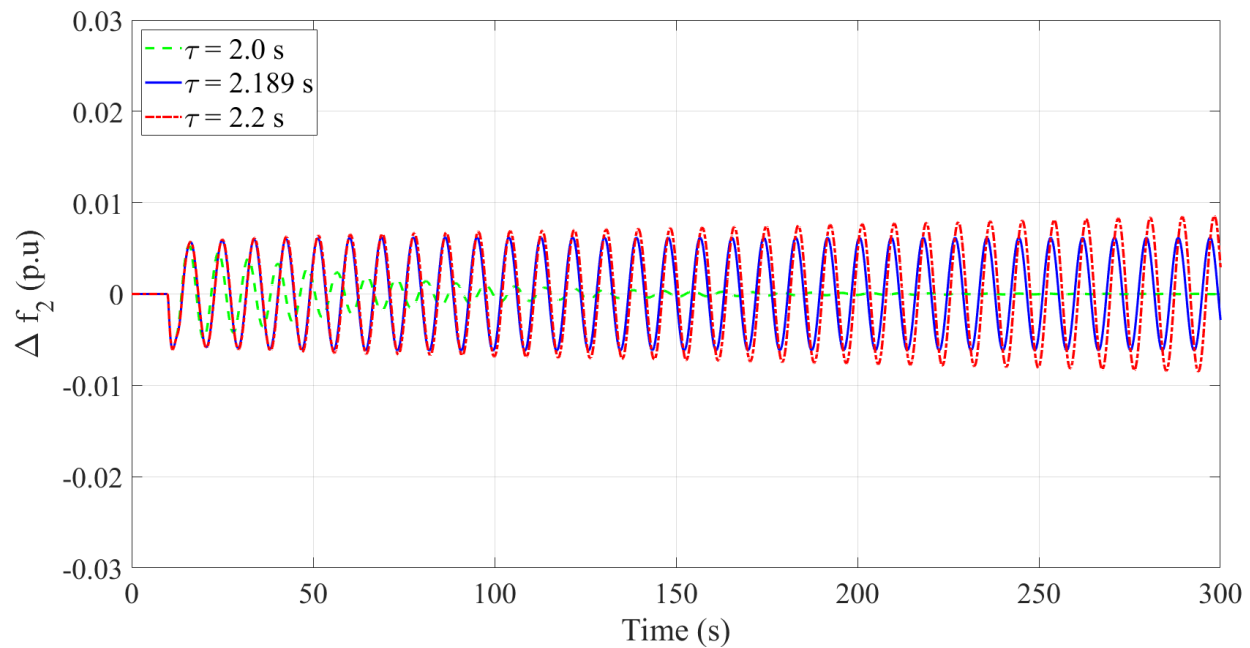


Figure 14. Frequency deviation for LFC-2: Δf_2 was measured while using $K_P = 0.4$ and $K_I = 0.6$.

Figures 13 and 14 depict the frequency response with time delay, τ , of 2.0 s, 2.189 s, and 2.2 s, for area 1 and area 2, respectively. It is obvious that the system is stable with $\tau = 2.0$ s and unstable with $\tau = 2.2$ s. Meanwhile, the system is marginally stable with $\tau = 2.189$ s. The percentage inaccuracy while employing the simulation-based DM is 0.000%. Figure 15 depicts the spectral radius against the frequency for $K_P = 0.4$ and $K_I = 0.6$. It was found that the crossing frequency, ω_c , was equal to 0.71530 rad/s with $\theta = 1.5658$ rad. By solving Equation (31), we obtain the DM equal to 2.189 s.

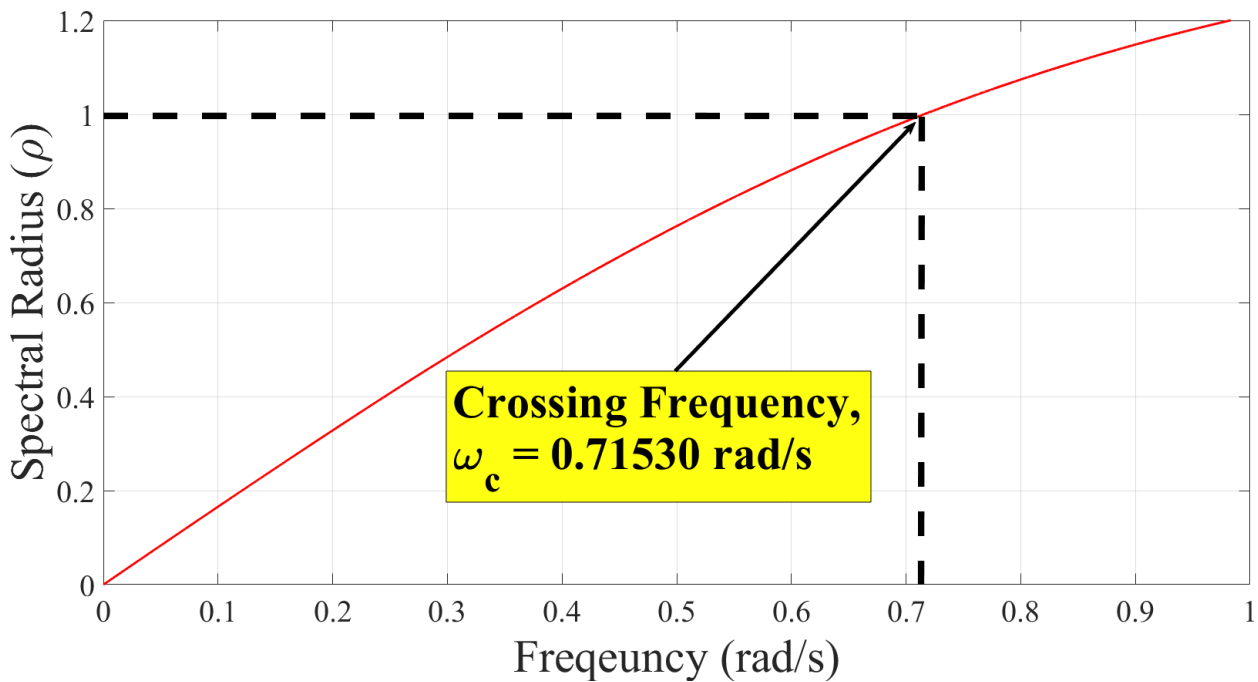


Figure 15. The spectral radius, ρ , against the frequency, ω , for $K_P = 0.4$ and $K_I = 0.6$.

Case study 3 with $K_P = 0.05$ and $K_I = 0.05$: The DM estimated using the method provided in reference [18] is 31.704 s, while it was 31.895 s with the proposed method. The frequency response of the two-area LFC system was illustrated in Figures 16 and 17, taking into account the impact of various time delays on area 1 and area 2, while setting $K_P = 0.05$ and $K_I = 0.05$.

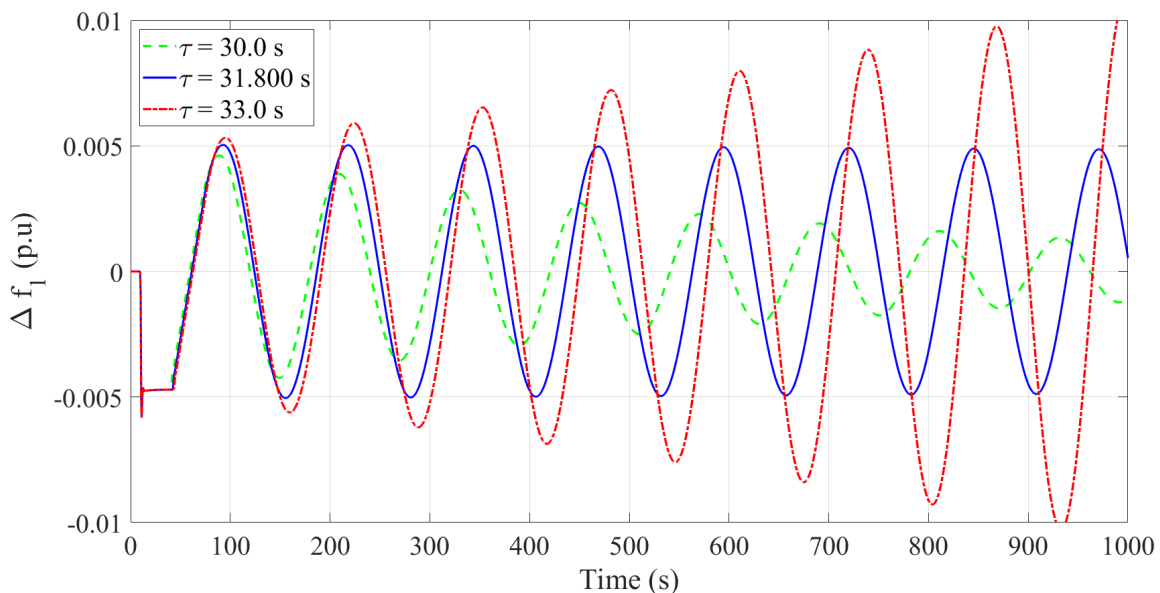


Figure 16. Frequency deviation for LFC–1: Δf_1 was measured while using $K_P = 0.05$ and $K_I = 0.05$.

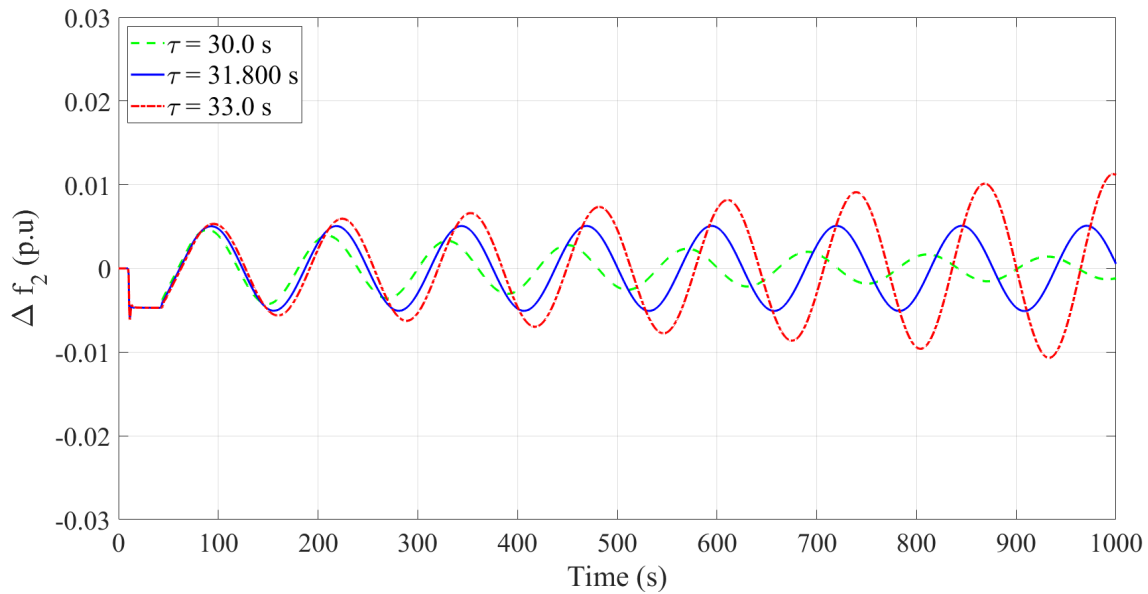


Figure 17. Frequency deviation for LFC–2: Δf_2 was measured while using $K_P = 0.05$ and $K_I = 0.05$.

Figures 16 and 17 depict the frequency response with time delay, τ , of 30.0 s, 31.800 s, and 33.0 s, for area 1 and area 2, respectively. It is obvious that the system is stable with $\tau = 30.0$ s and unstable with $\tau = 33.0$ s. Meanwhile, the system is marginally stable with $\tau = 31.800$ s. The percentage inaccuracy while employing the simulation-based DM is 0.2987%. Figure 18 depicts the spectral radius against the frequency for $K_P = 0.05$ and $K_I = 0.05$. It was found that the crossing frequency, ω_c , was equal to 0.05011 rad/s with $\theta = 1.5983$ rad. By solving Equation (31), we obtain the DM equal to 31.895 s.

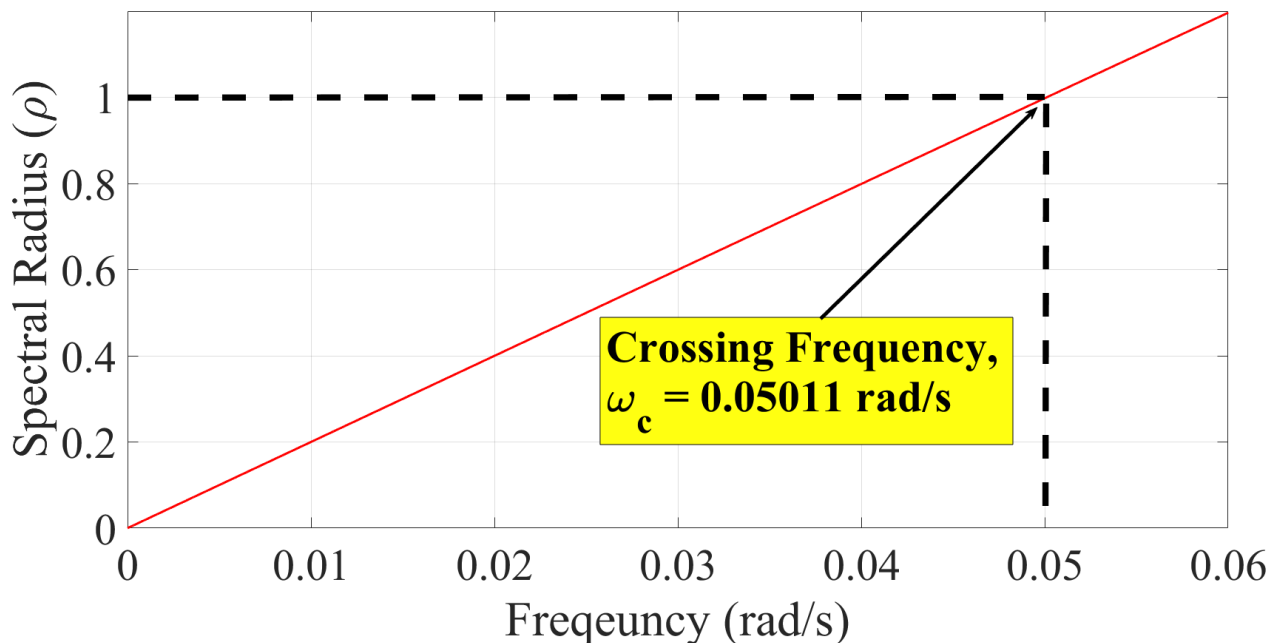


Figure 18. The spectral radius, ρ , against the frequency, ω , for $K_P = 0.05$ and $K_I = 0.05$.

Four other published methods were compared with the proposed method. As indicated in [28,29], the DM method produces less traditional results than the LMI method, but the LMI method has the advantage of handling delays that fluctuate over time. The proposed method is easier to execute, yet the DM results are similar to those obtained using the frequency domain techniques, as described in [18,19,28,29].

6. Conclusions

In this paper, a metaheuristic algorithm, namely the GWO, has been successfully employed to determine the optimal DM for a constant time delay of a two-area network. The optimisation of the spectral radius subjected to the optimal frequency formulated with the GWO is regarded as the most effective of all the techniques listed as it provides the minimum error of the spectral radius and hence optimises the best design variable of the crossing frequency such that an accurate result of DM can be obtained. A case study employing a two-area LFC system suggested that the proposed method is significantly superior in comparison to the others, as the sweeping range and sweeping step size method in the frequency domain method are no longer needed to determine the crossing frequency. In comparison to the previous methods, the time delay simulation showed that this novel technique provides precise delay margins with the smallest percentage error of 0.000%. In future work, a detailed case study of time-varying delay for load–frequency control with the proposed method will be implemented and compared with the most recently published methods.

Author Contributions: Conceptualisation, M.H.I., A.S.P. and A.K.; Formal analysis, M.H.I. and M.I.R.; Funding acquisition, A.S.P., M.N.D., K.H.L., S.Y., M.I.R. and T.W.A.; Investigation, M.H.I. and M.N.D.; Methodology, M.H.I. and A.S.P.; Supervision, A.S.P.; Validation, M.H.I., A.S.P., M.N.D., A.K. and M.I.R.; Visualisation, K.H.L. and S.Y.; Writing—original draft, M.H.I. and A.S.P.; Writing—review and editing, M.H.I., A.S.P., M.N.D. and M.I.R. All authors have read and agreed to the published version of the manuscript.

Funding: This research received no external funding.

Data Availability Statement: Not applicable.

Conflicts of Interest: The authors declare no conflict of interest.

References

1. Saadat, H. *Power System Analysis*; McGraw-Hill Companies: New York, NY, USA, 1999.
2. Xu, X.; Tomsovic, K. Application of Linear Matrix Inequalities for Load Frequency Control with Communication Delays. *IEEE Trans. Power Syst.* **2004**, *19*, 1508–1515.
3. Mak, K.H.; Holland, B.L. Migrating electrical power network SCADA systems to TCP/IP and Ethernet networking. *Power Eng. J.* **2002**, *16*, 305–311.
4. Gu, K.; Niculescu, S.I. Survey on Recent Results in the Stability and Control of Time-Delay Systems. *J. Dyn. Sys. Meas. Control.* **2003**, *125*, 158–165. [[CrossRef](#)]
5. Yan, S.; Gu, Z.; Park, J.H.; Xie, X.; Dou, C. Probability-density-dependent load frequency control of power systems with random delays and cyber-attacks via Circuital implementation. *IEEE Trans. Smart Grid* **2022**, *13*, 4837–4847. [[CrossRef](#)]
6. Yang, F.; He, J.; Pan, Q. Further Improvement on Delay-Dependent Load Frequency Control of Power Systems via Truncated B-L Inequality. *IEEE Trans. Power Syst.* **2018**, *33*, 5062–5071. [[CrossRef](#)]
7. Çelik, V.; Özdemir, M.T.; Lee, K.Y. Effects of Fractional-Order Pi Controller on Delay Margin in Single-Area Delayed Load Frequency Control Systems. *J. Mod. Power Syst. Clean Energy* **2018**, *7*, 380–389. [[CrossRef](#)]
8. Shen, L.; Xiao, H. Delay-Dependent Robust Stability Analysis of Power Systems with PID Controller. *Chin. J. Electr. Eng.* **2019**, *5*, 79–86. [[CrossRef](#)]
9. Jin, L.; Zhang, C.-K.; He, Y.; Jiang, L.; Wu, M. Delay-Dependent Stability Analysis of Multi-Area Load Frequency Control with Enhanced Accuracy and Computation Efficiency. *IEEE Trans. Power Syst.* **2019**, *34*, 3687–3696. [[CrossRef](#)]
10. Shen, C.; Li, Y.; Zhu, X.; Duan, W. Improved Stability Criteria for Linear Systems with Two Additive Time-Varying Delays via a Novel Lyapunov Functional. *J. Comput. Appl. Math.* **2020**, *363*, 312–324. [[CrossRef](#)]
11. Chen, W.; Gao, F.; Liu, G. New Results on Delay-Dependent Stability for Nonlinear Systems with Two Additive Time-Varying Delays. *Eur. J. Control.* **2021**, *58*, 123–130. [[CrossRef](#)]
12. Arunagirinathan, S.; Muthukumar, P. New Asymptotic Stability Criteria for Time-Delayed Dynamical Systems with Applications in Control Models. *Results Control. Optim.* **2021**, *3*, 100014. [[CrossRef](#)]
13. Feng, W.; Xie, Y.; Luo, F.; Zhang, X.; Duan, W. Enhanced Stability Criteria of Network-Based Load Frequency Control of Power Systems with Time-Varying Delays. *Energies* **2021**, *14*, 5820. [[CrossRef](#)]
14. Liu, X.; Shi, K.; Tang, L.; Tang, Y. Further Improvement on Stability Results for Delayed Load Frequency Control System via Novel Lkfs and Proportional-Integral Control Strategy. *Discret. Dyn. Nat. Soc.* **2022**, *2022*, 4798415. [[CrossRef](#)]
15. Li, Y.; Qiu, T.; Yang, Y. Delay-Dependent Stability Criteria for Linear Systems with Two Additive Time-Varying Delays. *Int. J. Control. Autom. Syst.* **2022**, *20*, 392–402. [[CrossRef](#)]

16. Khalil, A.; Swee Peng, A. A New Method for Computing the Delay Margin for the Stability of Load Frequency Control Systems. *Energies* **2018**, *11*, 3460. [[CrossRef](#)]
17. Khalil, A.; Laila, D.S. An Accurate Method for Computing the Delay Margin in Load Frequency Control System with Gain and Phase Margins. *Energies* **2022**, *15*, 3434. [[CrossRef](#)]
18. Sonmez, S.; Ayasun, S.; Nwankpa, C.O. An Exact Method for Computing Delay Margin for Stability of Load Frequency Control Systems with Constant Communication Delays. *IEEE Trans. Power Syst.* **2016**, *31*, 370–377. [[CrossRef](#)]
19. Thangaiah, J.M.; Parthasarathy, R. Delay-Dependent Stability Analysis of Power System Considering Communication Delays. *Int. Trans. Electr. Energy Syst.* **2016**, *27*, e2260. [[CrossRef](#)]
20. Ibrahim, M.H.; Ang, S.P.; Dani, M.N.; Rahman, M.I.; Petra, R.; Sulthan, S.M. Optimizing Step-Size of Perturb & Observe and Incremental Conductance MPPT Techniques Using PSO for Grid-Tied PV System. *IEEE Access* **2023**, *11*, 13079–13090. [[CrossRef](#)]
21. Shehata, A.A.; Tolba, M.A.; El-Rifaie, A.M.; Korovkin, N.V. Power System Operation Enhancement using a new hybrid methodology for optimal allocation of FACTS devices. *Energy Rep.* **2022**, *8*, 217–238. [[CrossRef](#)]
22. Sheikhzadeh-Baboli, P.; Assili, M. A hybrid adaptive algorithm for power system frequency restoration based on proposed emergency demand side management. *IETE J. Res.* **2021**, 1–13. [[CrossRef](#)]
23. Nadimi-Shahraki, M.H.; Taghian, S.; Mirjalili, S.; Abualigah, L.; Abd Elaziz, M.; Oliva, D. EWOA-OPF: Effective Whale Optimization Algorithm to Solve Optimal Power Flow Problem. *Electronics* **2021**, *10*, 2975. [[CrossRef](#)]
24. Nadimi-Shahraki, M.H.; Taghian, S.; Mirjalili, S.; Faris, H. MTDE: An effective multi-trial vector based differential evolution algorithm and its applications for engineering design problems. *Appl. Soft Comput.* **2020**, *97*, 106761. [[CrossRef](#)]
25. Nadimi-Shahraki, M.H.; Taghian, S.; Mirjalili, S. An improved grey wolf optimizer for solving engineering problems. *Expert Syst. Appl.* **2021**, *166*, 113917. [[CrossRef](#)]
26. Nadimi-Shahraki, M.H.; Moeini, E.; Taghian, S.; Mirjalili, S. DMFO-CD: A Discrete Moth-Flame Optimization Algorithm for Community Detection. *Algorithms* **2021**, *14*, 314. [[CrossRef](#)]
27. Nadimi-Shahraki, M.H.; Taghian, S.; Mirjalili, S.; Ewees, A.A.; Abualigah, L.; Abd Elaziz, M. MTV-MFO: Multi-Trial Vector-Based Moth-Flame Optimization Algorithm. *Symmetry* **2021**, *13*, 2388. [[CrossRef](#)]
28. Ramakrishnan, K. Delay-dependent stability criterion for delayed load frequency control systems. In Proceedings of the IEEE Annual India Conference (INDICON), Bangalore, India, 16–18 December 2016; pp. 1–6.
29. Jiang, L.; Yao, W.; Wu, Q.H.; Wen, J.Y.; Cheng, S.J. Delay-Dependent Stability for Load Frequency Control with Constant and Time-Varying Delays. *IEEE Trans. Power Syst.* **2012**, *27*, 932–941. [[CrossRef](#)]
30. Manikandan, S.; Kokil, P. Delay-Dependent Stability Analysis of Network-Based Load Frequency Control of One and Two Area Power System with Time-Varying Delays. *Fluct. Noise Lett.* **2019**, *18*, 1950007. [[CrossRef](#)]
31. Naduvathuparambil, B.; Valenti, M.C.; Feliachi, A. Communication delays in wide area measurement systems. In Proceedings of the Thirty-Fourth Southeastern Symposium on System Theory, Huntsville, Alabama, 18–19 March 2002; pp. 118–122.
32. Mirjalili, S.; Mirjalili, S.M.; Lewis, A. Grey Wolf Optimizer. *Adv. Eng. Softw.* **2014**, *69*, 46–61. [[CrossRef](#)]
33. Ibrahim, M.H.; Ang, S.P.; Hamid, Z.; Mohammed, S.S.; Law, K.H. A Comparative Hybrid Optimisation Analysis of Load Frequency Control in a Single Area Power System Using Metaheuristic Algorithms and LQR. In Proceedings of the 2022 International Conference on Green Energy, Computing, and Sustainable Technology (GECOST 2022), Miri, Sarawak, Malaysia, 26–28 October 2022; pp. 227–232.
34. Gu, K.; Kharitonov, V.L.; Chen, J. *Stability of Time-Delay Systems*; Springer: Berlin/Heidelberg, Germany, 2003.
35. Chen, J. On Computing the Maximal Delay Intervals for Stability of Linear Delay Systems. *IEEE Trans. Autom. Control* **1995**, *40*, 1087–1093. [[CrossRef](#)]
36. Chen, J.; Latchman, H.A. Frequency Sweeping Tests for Stability Independent of Delay. *IEEE Trans. Autom. Control* **1995**, *40*, 1640–1645. [[CrossRef](#)]
37. Chen, J.; Gu, G.; Nett, C.N. A New Method for Computing Delay Margins for Stability of Linear Delay Systems. In Proceedings of the IEEE 33rd Conference on Decision and Control, Lake Buena Vista, FL, USA, 14–16 December 1994; pp. 433–437.

Disclaimer/Publisher’s Note: The statements, opinions and data contained in all publications are solely those of the individual author(s) and contributor(s) and not of MDPI and/or the editor(s). MDPI and/or the editor(s) disclaim responsibility for any injury to people or property resulting from any ideas, methods, instructions or products referred to in the content.